ML3 Is a NEDD8- and Ubiquitin-Modified Protein[1][C][W][OPEN]

Jana P. Hakenjos, Sarosh Bejai, Quirin Ranftl, Carina Behringer, A. Corina Vlot, Birgit Absmanner, Ulrich Hammes, Stephanie Heinzlmeir, Bernhard Kuster, and Claus Schwechheimer*

Department of Plant Systems Biology (J.P.H., Q.R., C.B., C.S.) and Department of Proteomics and Bioanalytics (S.H., B.K.), Technische Universität München, 85354 Freising, Germany; Department of Plant Biology and Forest Genetics, Swedish University of Agricultural Sciences, 75007 Uppsala, Sweden (S.B.); Institute of Biochemical Plant Pathology, Helmholtz Zentrum München, 85764 Neuherberg, Germany (A.C.V.); and Department of Cell Biology and Plant Biochemistry, University of Regensburg, 93053 Regensburg, Germany (B.A., U.H.)

NEDD8 (NEURAL PRECURSOR CELL-EXPRESSED, DEVELOPMENTALLY DOWN-REGULATED PROTEIN8) is an evolutionarily conserved 8-kD protein that is closely related to ubiquitin and that can be conjugated like ubiquitin to specific lysine residues of target proteins in eukaryotes. In contrast to ubiquitin, for which a broad range of substrate proteins are known, only a very limited number of NEDD8 target proteins have been identified to date. Best understood, and also evolutionarily conserved, is the NEDD8 modification (neddylation) of cullins, core subunits of the cullin-RING-type E3 ubiquitin ligases that promote the polyubiquitylation of degradation targets in eukaryotes. Here, we show that Myeloid differentiation factor-2-related lipid-recognition domain protein ML3 is an NEDD8- as well as ubiquitin-modified protein in Arabidopsis (*Arabidopsis thaliana*) and examine the functional role of ML3 in the plant cell. Our analysis indicates that ML3 resides in the vacuole as well as in endoplasmic reticulum (ER) bodies. ER bodies are Brassicales-specific ER-derived organelles and, similar to other ER body proteins, ML3 orthologs can only be identified in this order of flowering plants. *ML3* gene expression is promoted by wounding as well as by the phytohormone jasmonic acid and repressed by ethylene, signals that are known to induce and repress ER body formation, respectively. Furthermore, ML3 protein abundance is dependent on NAI1, a master regulator of ER body formation in Arabidopsis. The regulation of *ML3* expression and the localization of ML3 in ER bodies and the vacuole is in agreement with a demonstrated importance of ML3 in the defense to herbivore attack. Here, we extend the spectrum of ML3 biological functions by demonstrating a role in the response to microbial pathogens.

The 8-kD protein ubiquitin is a well-studied modifier of eukaryotic proteins that is best known for targeting proteins conjugated to Lys-48-linked ubiquitin chains for degradation by the 26S proteasome (Komander and Rape, 2012). In addition, Lys-63-linked ubiquitin chains are required for targeting membrane proteins for degradation to the vacuole or the lysosome, and monoubiquitylation as well as polyubiquitylation events have been shown to control the activity, fate, or cellular behavior of proteins (Komander and Rape, 2012). E3 ubiquitin ligases recognize the ubiquitylation targets and promote ubiquitylation, while deubiquitylating enzymes are able to hydrolyze ubiquitin linkages (Hotton and Callis, 2008; Deshaies and Joazeiro, 2009; Komander et al., 2009). In addition to ubiquitin, several other ubiquitin-related proteins regulate cellular functions in eukaryotic cells, such as SMALL UBIQUITIN-LIKE MODIFIER (SUMO) or RELATED TO UBIQUITIN/NEURAL PRECURSOR CELL-EXPRESSED, DEVELOPMENTALLY DOWN-REGULATED (RUB/NEDD8 [herein NEDD8]; Rabut and Peter, 2008; Praefcke et al., 2012; Vierstra, 2012).

The fact that NEDD8 is the closest homolog of ubiquitin suggests that NEDD8 may have a similarly broad range of targets and activities as ubiquitin. However, only a very limited number of NEDD8-modified proteins has been identified to date (Rabut and Peter, 2008; Xirodimas, 2008; Ma et al., 2013). Best understood is the role of neddylation in regulating the cullin subunits of cullin-RING-type E3 ubiquitin ligases (Duda et al., 2008). Eukaryotic cells contain different types of cullin-RING ligases of varying architecture and varying substrate specificity (Duda et al., 2011; Harper and Tan, 2012). Cullin neddylation promotes E3 ligase complex activity as well as ubiquitylation by controlling E3 assembly and by inducing conformational rearrangements that promote substrate ubiquitylation (Duda et al., 2008). Additionally, a small number of animal proteins have been described as NEDD8 targets in recent years, but the biologically significance of their NEDD8 modification is only vaguely understood (Xirodimas et al., 2004, 2008; Rabut and Peter, 2008; Mahata et al., 2012; Noh et al., 2012; Ma et al., 2013).

ML proteins are defined as proteins with an MD-2-related lipid-recognition domain (Inohara and Nuñez,

[1] This work was supported by the Deutsche Forschungsgemeinschaft (grant nos. SCHW 751/9 and SCHW 751/11 to C.S. through SPP 1365 and to A.C.V. and U.H. through SFB924).

* Address correspondence to claus.schwechheimer@wzw.tum.de.

The author responsible for distribution of materials integral to the findings presented in this article in accordance with the policy described in the Instructions for Authors (www.plantphysiol.org) is: Claus Schwechheimer (claus.schwechheimer@wzw.tum.de).

[C] Some figures in this article are displayed in color online but in black and white in the print edition.

[W] The online version of this article contains Web-only data.

[OPEN] Articles can be viewed online without a subscription.

www.plantphysiol.org/cgi/doi/10.1104/pp.113.221341

2002). MD-2 is an extracellular binding partner of Toll-LIKE RECEPTOR4 (TLR4), and together, the two proteins mediate the response to bacterial lipopolysaccharides that are recognized as pathogen-associated molecular patterns that induce innate immunity responses in mammals (Viriyakosol et al., 2001; Kim et al., 2007; Park et al., 2009). The crystal structure of MD-2 has been resolved in its complex with TLR4 (Park et al., 2009). MD-2 consists of two antiparallel β-sheets that form a hydrophilic pocket for binding of the lipopolysaccharide ligand (Park et al., 2009). The protein Niemann-Pick-type C2 (NPC2) is another well-characterized ML protein. NPC2 binds cholesterol in the mammalian lysosome to initiate the transport of cholesterol across the lysosomal membrane via the activity of the transporter NPC1 (Xu et al., 2007). Loss of NPC1 and NPC2 leads to NPC disease, a rare lipid storage disorder where intracellular lipid transport is disrupted, leading to the accumulation of lipid products in late endosomes and lysosomes. The biochemical and cell biological functions of plant ML proteins are completely unresolved.

The endoplasmic reticulum (ER) exhibits a variety of shapes and movements in eukaryotic cells. The ER is composed of an extensive network of cisternae and tubules and can give rise to a range of ER-derived compartments that vary in size from 0.1 to 10 μm. ER bodies are such ER-derived compartments that were originally observed by electron microscopy in radish (*Raphanus sativus*) root cells as organelles of unknown origin (Bonnett and Newcomb, 1965). In Arabidopsis (*Arabidopsis thaliana*), these plant-specific spindle-shaped organelles were first recognized as ER-derived structures based on their ability to retain the ER marker protein green fluorescent protein (GFP)-HDEL, which carries an ER-targeting signal as well as an ER-retention signal (Haseloff et al., 1997; Ridge et al., 1999; Hayashi et al., 2001). In Arabidopsis, ER bodies can be found in seedlings and mature roots, and their formation can be induced in mature rosette leaves by methyl jasmonate (MeJA), a phytohormone induced in response to herbivore attack as part of the internal defense response and for signaling to neighboring plants. Mutant screens for ER body-deficient mutants have so far led to the identification of two proteins required for ER body formation, NAI1 and NAI2 (Matsushima et al., 2004; Yamada et al., 2008, 2009). NAI1 is a basic helix-loop-helix transcription factor essential for the formation of ER bodies in seedlings and roots that regulates the expression of the ER body proteins PYK10/BGLU23 and NAI2 (Matsushima et al., 2004). NAI2 is an ER body protein of unknown function with 10 glutamic acid-phenylalanine-glutamic acid repeats that has a signal peptide but, interestingly, no ER retention signal (Yamada et al., 2008, 2009). The purification of ER bodies from roots followed by mass spectrometric analysis resulted in the identification of the β-glucosidases PYK10/BGLU23 and BGLU21 as two major components of ER bodies (Matsushima et al., 2003; Nagano et al., 2008). The abundance of PYK10/BGLU23 correlates in different stages of plant growth and development with the absence, induction, and presence of ER bodies, and mutations in PYK10/BGLU23 and BGLU21 affect ER body size positively (Nagano et al., 2009). PYK10/BGLU23, therefore, is thought to be a major and possibly specific component of ER bodies.

At present, ER bodies have only been observed in species of the order Brassicales, which includes Arabidopsis and *Brassica rapa*. The observation that ER bodies are induced by jasmonate has given rise to the hypothesis that ER bodies may participate in plant-pathogen responses (Matsushima et al., 2002, 2004; Hara-Nishimura and Matsushima, 2003). ER bodies may form in response to pathogen attack to release hydrolytic enzymes to fend off the herbivore after wounding (e.g. by hydrolyzing inactive secondary metabolites such as scopolin into active scopoleptin; Ahn et al., 2010). In support of this hypothesis, a deletion in the *NAI1* promoter was associated with increased susceptibility to the mutualistic fungus *Piriformospora parasitica* (Sherameti et al., 2008). Jacalin-related lectins and GDSL lipase-like proteins may contribute to such defense responses by forming complexes with PYK10/BGLU23. Also, ML3 has recently been linked to defense signaling in a study that showed that *ml3* mutants are hypersensitive to herbivore attack (Fridborg et al., 2013).

In this study, we characterize the ML domain protein ML3. We and others have previously identified ML3 as a putatively NEDD8-modified protein (Hakenjos et al., 2011; Hotton et al., 2012). Here, we show that ML3 is indeed a NEDD8- as well as a ubiquitin-conjugated protein in planta. ML3 is also conjugated to ubiquitin, but it can also noncovalently interact with both ubiquitin family proteins. *ML3* expression is induced after wounding and herbivore attack as well as by treatment with the hormone MeJA. ML3 localizes to the vacuole and to ER bodies, and *ml3* mutants are defective in their response not only to herbivores but also to microbial pathogens.

RESULTS

ML3 Is a Novel NEDD8- and Ubiquitin-Modified Protein

We have previously used transgenic lines that express hemagglutinin-STREP-tagged NEDD8 (HSN) under the control of a dexamethasone-inducible gene expression system to isolate NEDD8-modified proteins from Arabidopsis (Aoyama and Chua, 1997; Hakenjos et al., 2011). Using the STREP affinity tag, we were able to purify a number of proteins as putative NEDD8 conjugates from total protein extracts prepared from an HSN line (Hakenjos et al., 2011). However, our experimental strategy suffered from the weakness that the choice of the purification tag only allowed purifying HSN conjugates under native conditions, so that we may have recovered proteins that are themselves not NEDD8 modified but interact with such conjugates. Therefore, we set out to examine a subset of these putative NEDD8 conjugates more critically with regard to their

NEDD8 modification. In this context, we also generated *MYC-ML3* lines for the expression of a MYC-tagged variant of the putative NEDD8 conjugate ML3 in the HSN transgenic background. Following immunoprecipitation of the MYC-ML3 fusion protein (calculated mass of 28.3 kD), we could detect the protein with an anti-MYC antibody in two prominent forms of approximately 32 and 44 kD. Detection of HSN conjugates with an anti-hemagglutinin (HA) antibody then revealed the presence of at least two additional HSN-conjugated forms of MYC-ML3 of approximately 55 kD, suggesting that a minor fraction of MYC-ML3 is indeed NEDD8 modified (Fig. 1A). Since our further analysis of the protein sequence revealed that ML3 carries an N-terminal signal peptide that should be proteolytically cleaved during protein transport, we also generated a construct for the expression of a C-terminally tagged ML3, *ML3-YFP-HA* (where YFP stands for yellow fluorescent protein; calculated mass of 51 kD). Following immunoprecipitation of ML3-YFP-HA, we could again confirm that ML3 is NEDD8 modified, because a fraction of immunoprecipitated ML3-YFP-HA was also recognized by an antibody directed against the endogenous NEDD8 protein, which detected a higher mass form of ML3-YFP-HA that could be explained by the conjugation of the 8-kD NEDD8 (Fig. 1B). We thus concluded that ML3 is indeed a NEDD8-modified protein.

Following immunoprecipitation and mass spectrometry (MS), we subsequently identified Lys-137 as at least one Lys residue of immunoprecipitated ML3-YFP-HA that carried the di-Gly footprint that is retained on NEDD8- and ubiquitin-modified proteins after trypsin digestion (Supplemental Fig. S1). We then mutagenized Lys-137 and subsequently all other Lys residues of ML3 to Arg with the goal of obtaining a nonneddylatable ML3 variant. However, the NEDD8 modification of ML3 was detected in each of these ML3 mutant variants, indicating that NEDD8 may be attached to multiple or to variant Lys residues in the wild type or the mutated ML3 proteins (Supplemental Fig. S2). The conclusion that ML3 may be neddylated at multiple residues is also supported by our observation that frequently more than one neddylated form of ML3 was apparent in immunoblots following the immunoprecipitation of ML3 and the detection of HSN or endogenous NEDD8 (Fig. 1). In summary, these data suggest that ML3 may be modified by multiple NEDD8 molecules.

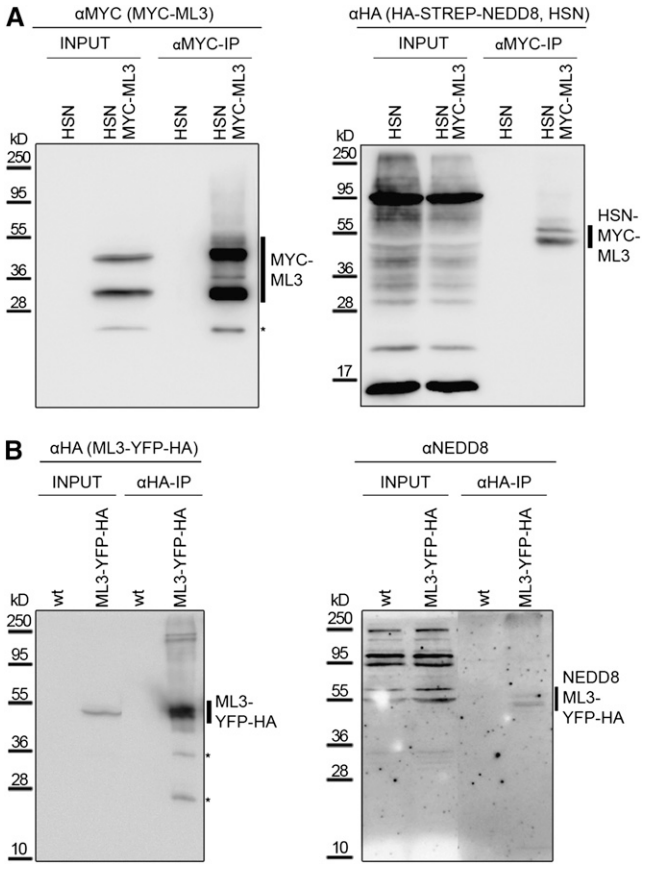

Figure 1. ML3 is a NEDD8-modified protein. A, Results of an immunoprecipitation of MYC-ML3 from 7-d-old Arabidopsis seedlings with anti-MYC agarose. Left panel, immunoblot with anti-MYC of the input control (45 μg of total protein) and the immunoprecipitate (IP) of MYC-ML3; right panel, immunoblot with anti-HA of the input and the anti-MYC immunoprecipitate. MYC-ML3 is detected in the form of two abundant variants of approximately 32 and 44 kD. B, Results of an immunoprecipitation of ML3-YFP-HA from 7-d-old Arabidopsis seedlings. Left panel, immunoblot with anti-HA of the input control (45 μg of total protein) and immunoprecipitate of ML3-YFP-HA; right panel, immunoblot with anti-NEDD8 of the input and the anti-HA immunoprecipitate. wt, Wild type. Asterisks indicate apparent degradation products.

ML3 May Be a NEDD8- and Ubiquitin-Binding Protein

To be able to detect endogenous ML3 protein, we raised an anti-ML3 peptide antibody that readily detected the 18-kD (calculated) ML3 protein in total protein extracts from wild-type plants. Since we detected HSN-conjugated ML3 following HSN immunoprecipitation, we concluded that also endogenous ML3 is NEDD8 modified (Fig. 2A). We then used the neddylation inhibitor MLN4924 to test whether the modification of ML3 was dependent on the activity of the NEDD8 E1 conjugation enzyme (Hakenjos et al., 2011). Indeed, ML3 neddylation was reduced following a pretreatment of the plants with MLN4924, suggesting that ML3 is NEDD8 modified by the established NEDD8 conjugation pathway (del Pozo et al., 1998, 2002; del Pozo and Estelle, 1999; Woodward et al., 2007; Supplemental Fig. S3).

Interestingly, when we immunoprecipitated NEDD8 using the tagged HSN fusion variant, we noted that anti-ML3 did not only detect ML3 as a neddylated HSN conjugate but also ML3 in its apparent unmodified form (Fig. 2A). Similar results were obtained following immunoprecipitations of HSN conjugates from the MYC-ML3 transgenic line (Supplemental Fig. S4). In these immunoprecipitations, we detected specifically the

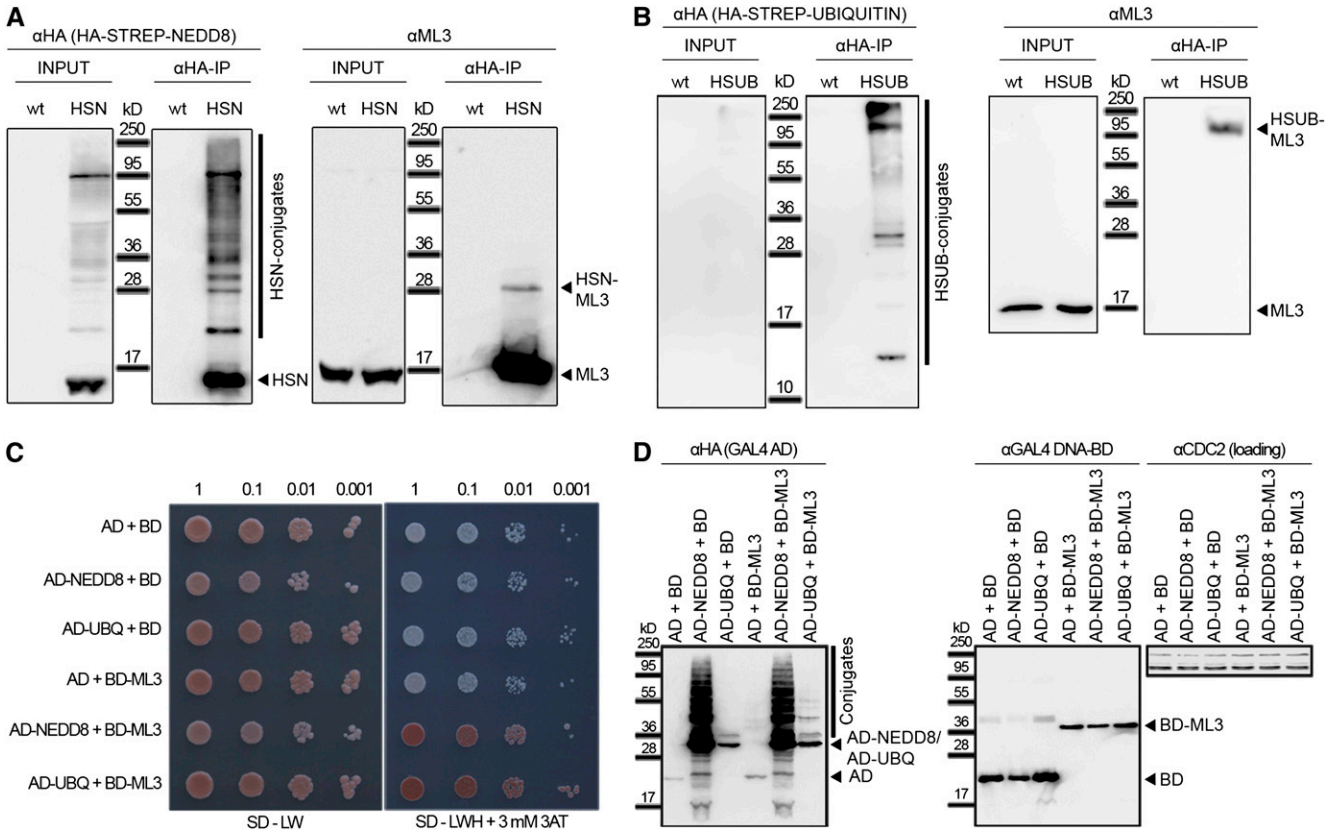

Figure 2. ML3 is conjugated to and binds to NEDD8 and ubiquitin. A and B, Results of immunoprecipitations of HSN (A) or HSUB (B) from 7-d-old Arabidopsis seedlings with anti-HA agarose. Left panel, immunoblot with anti-HA of the input control (45 μg of total protein) and immunoprecipitate (IP) of HSN or HSUB; right panel, immunoblot with anti-ML3 of the input (45 μg of total protein) and the anti-HA immunoprecipitate. wt, Wild type. C, Result of a yeast two-hybrid interaction analysis with GAL4 DNA-binding domain (BD) and activation domain (AD) fusion constructs testing for the interaction of ML3 with NEDD8 and ubiquitin (UBQ). Yeast was grown on selection media lacking leucine and tryptophane (SD-LW) for growth control and on media additionally lacking histidine and 3-aminotriazole (SD-LWH + 3 mM 3AT) to check for interaction. D, Protein expression analysis of the various yeast strains shown in C. GAL4 AD fusions are detected with anti-HA; DB fusions are detected with anti-GAL4 DNA-BD; equal protein loading is controlled for with anti-CDC2. Note the presence of numerous AD-NEDD8 conjugates in the anti-HA immunoblot. [See online article for color version of this figure.]

32-kD variant of MYC-ML3 and not the 44-kD higher mass form (Supplemental Fig. S4), and we took this finding as an indirect indication that the 32-kD variant detected in *MYC-ML3* lines represents the neddylatable form of *MYC-ML3* (Fig. 1). The 44-kD form, in turn, may represent a posttranslationally modified form that cannot be neddylated and that could result from the protein's N-terminal signal peptide being blocked by the MYC tag.

We reasoned that the appearance of unconjugated ML3 may be the result of an enzymatic deconjugation of HSN-ML3 during the immunoprecipitation procedure. Alternatively, ML3 may bind to NEDD8 or to NEDD8 conjugates in a noncovalent manner. The latter view was supported by an EMBL-European Nucleotide Archive database entry for ML3 that described the protein as a yeast two-hybrid interactor of a ubiquitin pentamer (ABH03542) as well as by the fact that abundant amounts of ML3 were precipitated in the immunoprecipitation experiments that, in our view, could not be explained by the small amounts of NEDD8-modified ML3 detected in immunoblots after HSN immunoprecipitations.

To test whether ML3 can be covalently linked to ubiquitin, we carried out immunoprecipitations from transgenic lines that express HSUB, a construct analogous to HSN for the inducible expression of an HA-STREP-tagged ubiquitin. Indeed, we could detect ML3 also in the form of a high-mass ubiquitin conjugate of approximately 150 kD in the HSUB immunoprecipitates (Fig. 2B). Thus, we concluded that ML3 is a NEDD8-conjugated as well as a ubiquitin-conjugated protein in vivo. While we detected small amounts of the apparently unmodified ML3 variant also in several HSUB-ML3 purifications (data not shown), this form of ML3 was absent in others. Therefore, we reasoned that the copurification of the unmodified ML3 is the result of a deconjugation of ML3 from HSUB-ML3 (e.g. by deubiquitylating enzymes) that occurred during the immunoprecipitation of HSUB

conjugates. Similarly, ML3 may be deconjugated from HSN-ML3 in the respective immunoprecipitations of HSN.

To test whether NEDD8 and ubiquitin can interact with ML3 also in a noncovalent manner, we tested their interactions using the yeast two-hybrid system. Indeed, this interaction analysis revealed that ML3 readily interacts with both ubiquitin family proteins in the yeast system (Fig. 2C). Analysis of the expression of the fusion proteins in yeast confirmed that all proteins were expressed, but interestingly, also that the GAL4 activation domain fusion protein fused to NEDD8 (AD-NEDD8) was conjugated to a broad range of proteins in the yeast host (Fig. 2D). No such conjugates could be detected in the case of activation domain-ubiquitin (AD-UBQ), possibly reflecting the fact that such ubiquitin conjugates are directly targeted for proteasomal degradation.

ML3 Belongs to the MD-2-Related Lipid-Recognition Domain Family of Proteins

ML3 is encoded by the Arabidopsis gene *AT5G23820*. ML3 has two closely related putative paralogs adjacent to the *ML3* locus on chromosome 5 of the Arabidopsis genome, namely ML5 (AT5G23840; 76% amino acid identity to ML3) and ML6 (AT5G23830; 73% identity; Fig. 3A). Additionally, these three ML domain proteins share sequence homology with a number of proteins from Arabidopsis and *B. rapa* and with other proteins from non-Brassicaceae species, such as the dicots tomato (*Solanum lycopersicum*), grapevine (*Vitis vinifera*), and soybean (*Glycine max*) and the monocots rice (*Oryza sativa*) and *Brachypodium distachyon* (Fig. 3; Supplemental Figs. S5 and S6). Although the genomes of both Arabidopsis and *B. rapa* encode three ML3-like proteins, namely Arabidopsis ML3, ML5, and ML6 and *B. rapa* Bra020976, Bra028884, and Bra011987, the three ML3 paralogs of each species are more closely related to each other than to the proteins from the respective other species, suggesting that they originated from independent duplication events (Fig. 3B; Supplemental Fig. S5).

Based on the current annotation of these proteins, the vast majority of ML3-related proteins from Arabidopsis and *B. rapa* contains an N-terminal signal peptide, which suggests that these proteins are directed to the ER and from there targeted to the vacuole or the secretory pathway (Fig. 3A; Petersen et al., 2011). The remaining part of these ML proteins has sequence homology with the lipid recognition domain of the mammalian ML domain proteins MD-2 and NPC2 (Supplemental Fig. S6; Viriyakosol et al., 2001; Inohara and Nuñez, 2002). However, the restricted homology within this domain does not allow drawing any conclusions on the binding specificity of any of the Arabidopsis proteins (Supplemental Fig. S6). Based on their homology to MD-2, the members of this protein family were previously classified as ML proteins; however, none of the plant ML domain proteins have been characterized at the biochemical, cell biological, or functional level as yet (Inohara and Nuñez, 2002). We also noted with interest that proteins closely related to ML3 can only be found in Brassicales species, including Arabidopsis and *B. rapa*, or inversely that these proteins are seemingly absent from the genomes of non-Brassicales dicots, monocots, the moss *Physcomitrella patens*, and the lycophyte *Selaginella moellendorffii* (Fig. 3B; Supplemental Fig. S5).

Identification of *ml3* Mutants

In order to understand the biological function of ML3, we examined two putative *ml3* alleles with transfer DNA (T-DNA) insertions in the *ML3* open reading frame and 3′ untranslated region, *ml3-3* (SALK_001255) and *ml3-4* (SAIL_182_G07; Fig. 4A). Our subsequent analysis of ML3 protein abundance in the *ml3-3* and *ml3-4* mutants showed that ML3 protein cannot be detected in *ml3-3* and *ml3-4* (Fig. 4B). While this work was in progress, two additional mutant alleles, *ml3-1* (SALK_059591) and *ml3-2* (SALK_091638), were described as part of another study of genes related to the defense to herbivores (Fridborg et al., 2013). While this study had associated semidwarfed growth with *ml3-1* and *ml3-2*, we could not detect such a phenotype in *ml3-3* and *ml3-4* when grown in continuous light growth conditions (Fig. 4C). For our further work, we considered the exon insertion allele *ml3-3* as the prototypical *ml3* mutant allele.

ML3 Resides in the Vacuole and in ER Bodies

In order to understand the intracellular distribution of ML3, we generated transgenic lines that express ML3 as a fusion with the fluorescent protein mCherry under the control of a 2-kb *ML3* promoter fragment (*ML3p:ML3-mCherry*). Our analysis of transgenic lines expressing this protein revealed that the protein accumulates in the vacuole as well as in rod-shaped structures that we identified as ER bodies based on their size and shape. This was also supported by their partial colocalization with the marker Q4, which highlights the membranes of ER bodies as well as the cellular ER network, and by their exclusive presence in the seedling epidermis and the cotyledons (Fig. 5A). The ER body localization of ML3 was also verified in lines expressing ML3-YFP from the *ML3* promoter fragment (*ML3p:ML3-YFP*; Fig. 5B). In turn, *ML3p:ML3-YFP* lines did not allow us to visualize the vacuolar localization of ML3 (Fig. 5C), most likely due to the fact that GFP and the closely related YFP are degraded in the vacuole (Tamura et al., 2003). To confirm the vacuole and ER body localization for the endogenous ML3, we purified vacuoles and performed a subcellular fractionation based on previously established protocols (Matsushima et al., 2003; Robert et al., 2007). In these analyses, we identified endogenous ML3 in vacuolar preparations from 14-d-old seedlings where ML3 cofractionated with the marker vacuolar ATPase (Fig. 5D). To resolve ER bodies, we performed centrifugation of protein extracts at 1,000*g* from a transgenic line expressing

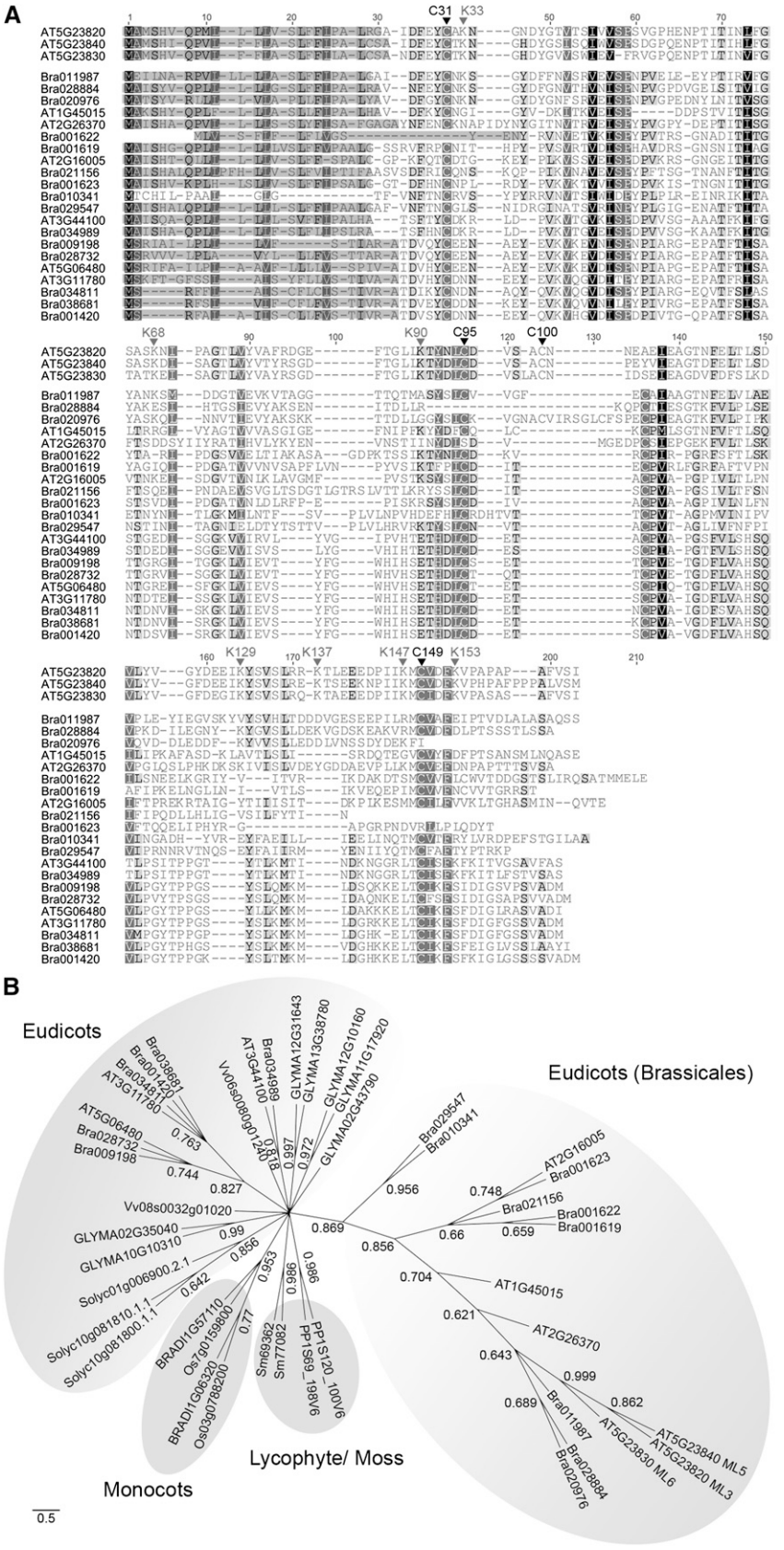

Figure 3. ML3 is a conserved plant protein that belongs to the family of MD2-related proteins. A, ClustalOmega alignment of ML3 (AT5G23820) and its homologous sequences retrieved from Arabidopsis (AT) and *B. rapa* (Bra). The N-terminal signaling peptide (shaded) was predicted with SignalP 4.0 (Petersen et al., 2011). The seven Lys (K) residues that are conserved in ML3, ML5, and ML6 but also in other MD-2 domain proteins are indicated. Cys residues required for the formation of two intramolecular Cys bridges that have been reported for MD-2 also appear to be conserved in the plant proteins. An exception are the Arabidopsis proteins ML3, ML5, and ML6 that lack one of these conserved Cys residues; Cys-100 (ML3) may functionally replace this missing Cys residue. B, Phylogenetic tree of the MD-2 domain proteins related to ML3 from Arabidopsis (AT) and *B. rapa* (Bra) as shown in A as well as from the moss *P. patens* (PP), soybean (GLYMA), rice (Os), *B. distachyon* (BRADI), grapevine (Vv), and tomato (Solyc). Protein sequences were retrieved at www.ensembl.org. The phylogenetic tree was generated with the conserved MD-2 domain and is drawn to scale. The underlying alignment is shown in Supplemental Figure S5. Bootstrap values are indicated by each node. Bar = 0.2 amino acid substitutions per site.

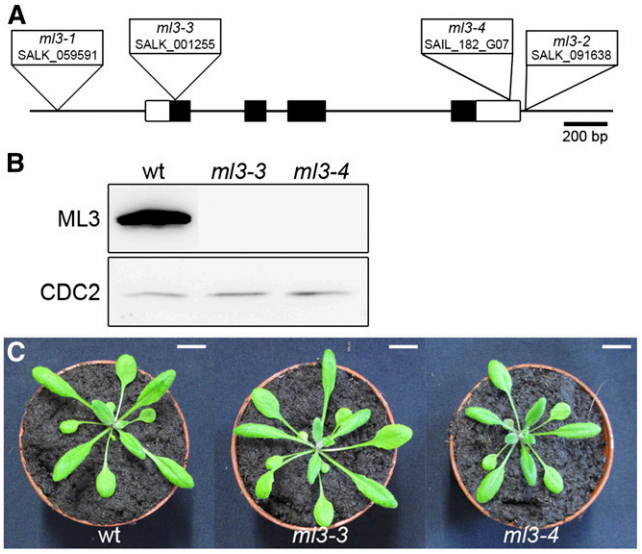

Figure 4. Identification of *ml3* mutants. A, Schematic view of the *ML3* locus and positioning of the respective T-DNA insertion mutant alleles. Black boxes, exons; white boxes, untranslated regions; line, untranscribed upstream and downstream regions as well as introns. B, Immunoblot from protein extracts of 7-d-old wild-type (wt) and *ml3-3* as well as *ml3-4* mutant seedlings. C, Photograph of 1-month-old plants of the wild type and the alleles *ml3-3* and *ml3-4*. There are no apparent growth differences between the wild type and these *ml3* mutant alleles. Bars = 1 cm. [See online article for color version of this figure.]

the ER marker GFP-HDEL. Interestingly, ML3 could not be retrieved in the 1,000*g* fraction that contains the ER bodies, suggesting that native ML3 may not reside in ER bodies and that the ER body localization of ML3-mCherry may be an artifact of the protein fusion (Fig. 5D). In turn, we detected ML3 in the soluble S100 fraction, in line with its localization to the vacuole. Identical fractionations of the YFP-tagged ML3-YFP-HA, however, confirmed the proposed ER body localization also for ML3-YFP-HA (Fig. 5E). In summary, we concluded that ML3 is a vacuolar protein that may potentially also reside in ER bodies.

The vacuolar localization of ML3 observed here is in agreement with the results of a previously published proteomics study that had identified ML3 in vacuoles of Arabidopsis plants (Carter et al., 2004). Interestingly, ML3 was also identified in another proteomics study that aimed at the identification of proteins that are secreted in response to treatments with the plant hormone salicylic acid (SA; Oh et al., 2005). Since ML3 had been shown to be involved in the plant's defense to herbivore attack, which induces SA responses (Oh et al., 2005; Bejai et al., 2012; Fridborg et al., 2013), we reasoned that ML3 may relocalize to the extracellular space in response to activation of the SA pathway. While we noticed indeed a presence of ML3-mCherry after SA treatment (2 h), our subsequent analyses indicated that this is likely artifactual, because it was also found with the unrelated vacuolar lumen marker sp-RFP-AFVY (Hunter et al., 2007) and because ML3-mCherry secretion was the apparent result of pH changes and did not occur in buffered solutions or in the presence of mannitol (Supplemental Fig. S7).

ML3 Is Coexpressed with ER Body Genes and in Response to NAI1

To gain further insight into the function of ML3, we searched for genes that are coexpressed with *ML3*. Through the analysis of all available microarray data sets deposited in Genevestigator, we identified a number of coexpressed genes and noticed with interest that eight genes among the first 20 coregulated genes had a demonstrated or proposed function in ER body biology or formation (Table I). This set of coregulated genes included *NAI1*, a basic helix-loop-helix transcription factor essential for ER body formation, as well as proposed NAI1 target genes such as *NAI2* and *PYK10* (Matsushima et al., 2004). Since *ML3* had also been found to be differentially expressed in a comparison of *nai1* mutants with the wild type, we hypothesized that NAI1 may regulate *ML3* gene expression. This assumption found support in our observation that *ML3* expression was strongly reduced in the *nai1* mutant *nai1-3* (GK-136G06-012754; Fig. 6A). Since *nai1* mutants are defective in the formation of ER bodies and since we had identified ML3

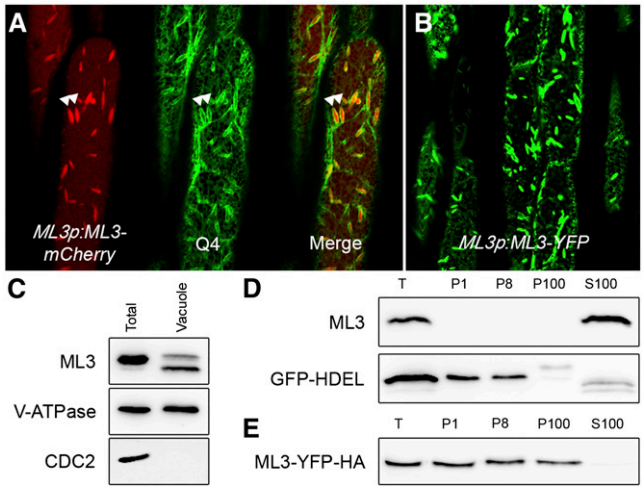

Figure 5. ML3 is a vacuolar and ER body-localized protein. A, Confocal microscopy images of hypocotyl epidermal cells from 5-d-old seedlings expressing ML3-mCherry (left panel) from the *ML3* promoter (*ML3p*) and the ER and ER body membrane marker Q4 (middle panel). The merged image is shown in the right panel. The double arrowheads point at ER bodies. B, Confocal image of the expression of ML3p:ML3-YFP in the epidermis of a 5-d-old Arabidopsis seedling. C, Immunoblots of total protein extracts and a vacuole preparation from 14-d-old Arabidopsis wild-type seedlings. D and E, Immunoblots of a total protein extract and pellet fractions obtained after differential centrifugation of a protein extract prepared from 7-d-old GFP-HDEL (D) and ML3-YFP-HA (E) transgenic seedlings after centrifugation at 1,000*g* (P1), 8,000*g* (P8), or 100,000*g* (P100). S100, Soluble supernatant after centrifugation at 100,000*g*; T, total protein extract.

as a putative ER body protein, we questioned whether the apparent absence of ML3 protein in the *nai1* mutant was the consequence of the absence of NAI1 as its transcriptional regulator or the indirect consequence of the absence of ER bodies in this mutant. To address this question, we examined ML3 protein abundance also in *nai2-2* (SALK_005896) and *nai2-3* (SALK_043149) mutants. NAI2 is a protein of unknown function in ER bodies that is essential for ER body formation but does not have an apparent function related to transcriptional regulation (Yamada et al., 2008). Importantly, ML3 protein was detectable in *nai2* but, as mentioned above, absent in *nai1*, suggesting that the absence of ML3 in *nai1* is the result of the absence of the transcriptional regulation by NAI1 rather than the indirect consequence of the absence of ER bodies (Fig. 6C). Inversely, we found no evidence that the absence of ML3 in *ml3-3* has an influence on the formation of ER bodies (Supplemental Fig. S8).

NAI1 is essential for ER body formation, which is promoted by the plant hormone jasmonic acid (JA; Matsushima et al., 2004). It has previously been established that *NAI1* transcription is induced by MeJA and reduced in response to ethylene (Matsushima et al., 2004). We hypothesized that *ML3* expression should follow this pattern of transcriptional regulation of *NAI1* if it was a direct NAI1 transcription target. Indeed, we found that the abundance of *ML3* and *NAI1* as well as the ER body-resident *PYK10* gene is induced by MeJA treatments and suppressed by concomitant treatments with the ethylene precursor 1-aminocyclopropane-1-carboxylic acid, which is converted into the gaseous ethylene hormone when taken up by the plant (Fig. 7A). This finding thus supported the notion that *ML3* is a direct NAI1 transcription target.

MeJA is produced in plants in response to wounding by herbivore pathogens. The knowledge about the regulation of NAI1 and ER body formation by MeJA has given rise to the concept that ER bodies may play a role in the response to pathogens (Yamada et al., 2011). Interestingly, we found *ML3* expression in the *ML3p*:*ML3-mCherry* lines to be restricted to the epidermis, an observation that could be considered in support of the proposed function in biotic and abiotic interactions with the environment (Fig. 7B). To assess the possibility of a putative regulation of *ML3* expression by wounding, we generated transgenic lines that express the reporter *GUS* under the control of a 2-kb *ML3* promoter fragment. Following the wounding of leaves of transgenic lines expressing this *ML3p*:*GUS* construct, we observed indeed increased staining at the sites of wounding as well as systemic spreading of the signal over the entire blade of the wounded leaf (Fig. 7C). Since ML3 had previously been analyzed in the context of herbivore defense, we also challenged *ML3p*:*GUS* lines with second instar larvae of the herbivore *Spodoptera littoralis* and found clear evidence for *ML3* induction at the sites of wounding after insect feeding (Fig. 7D). In summary, these findings support that notion that *ML3* is a transcription target downstream from NAI1

Table I. *List of genes identified by Genevestigator as being coexpressed with ML3*

Arabidopsis Genome Initiative Identifier	Score	Gene Name	Reference
AT5G23820	1.000	ML3	Nagano et al. (2008)
AT3G16410, AT3G16390, AT3G16400	0.748	NITRILE-SPECIFIER PROTEIN4, NITRILE-SPECIFIER PROTEIN3, and NITRILE-SPECIFIER PROTEIN1	Kuchernig et al. (2012)
AT3G16430, AT3G16420	0.737	JACALIN-RELATED LECTIN31 and JACALIN-RELATED LECTIN30	Nagano et al. (2008) Nagano et al. (2005) Matsushima et al. (2004)
AT1G54010, AT1G54000	0.701	GDSL LIPASE-LIKE PROTEIN22	Nagano et al. (2005)
AT3G09260	0.694	PYK10	Ogasawara et al. (2009) Matsushima et al. (2004) Matsushima et al. (2003)
AT2G39310	0.660	JACALIN-RELATED LECTIN22	Nagano et al. (2008)
AT3G15950	0.655	NAI2	Nagano et al. (2008)
AT1G31710	0.653	Copper amine oxidase family protein	
AT3G16460	0.653	JACALIN-RELATED LECTIN34	
AT2G22170	0.647	PLAT DOMAIN PROTEIN2	
AT2G22770	0.640	NAI1	Matsushima et al. (2004)
AT1G76790	0.639	IGOMT5	Pfalz et al. (2011)
AT3G16450	0.635	JACALIN-RELATED LECTIN33	Nagano et al. (2008)
AT5G15230	0.634	GAST1 PROTEIN HOMOLOG4	
AT3G20370	0.621	TRAF-like family protein	
AT5G44020	0.607	HAD superfamily, subfamily IIIB acid phosphatase	
AT4G27860	0.599	MEMBRANE OF ER BODY1	Yamada et al. (2013)
AT3G54400	0.597	Eukaryotic aspartyl protease family protein	
AT4G23670	0.596	Polyketide cyclase/dehydrase and lipid transport superfamily protein	
AT3G63200	0.596	PATATIN-LIKE PROTEIN9	

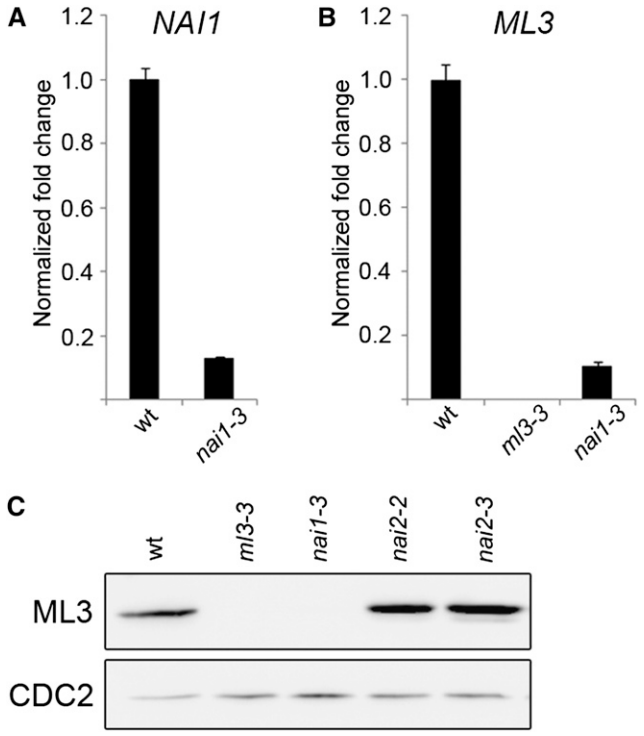

Figure 6. *ML3* expression is promoted by the ER body regulator NAI1. A and B, Results of qRT-PCR analyses testing for *NAI1* (A) and *ML3* (B) transcript abundance in 7-d-old wild-type (wt) and *nai1-3* or *ml3-3* mutant seedlings. C, Immunoblot with anti-ML3 testing for the abundance of ML3 in total protein extracts (45 μg) prepared from 7-d-old wild-type seedlings as well as *nai1* and *nai2* mutant seedlings. Anti-CDC2 served as a loading control for this experiment.

that is induced in response to wounding and herbivore attack.

A Role for ML3 in the Pathogen Response

ER bodies have been proposed to function in pathogen responses (Yamada et al., 2011). For this reason, we were interested in examining the performance of *ml3* mutants after challenge with the fungal pathogen *Alternaria brassicicola* and the pathogenic bacterium *Pseudomonas syringae* DC3000. *A. brassicicola* is a necrotrophic fungus that induces cell death upon infection. In comparison with the wild type, in which cell lesions were largely restricted to the inoculation spots, *ml3* mutants showed increased susceptibility, visible by the increased spreading of necrosis away from the site of infection at 5 d after infection (Fig. 8, A and B). Lesion expansion was associated with an increase of fungal DNA in *ml3* mutants and was partially similar to the responses of the camalexin-deficient mutant *pad3-1* that has previously been shown to possess enhanced susceptibility to *A. brassicicola* (Schuhegger et al., 2006). In the case of the *P. syringae* infection experiments, we detected reduced pathogen growth 6 d post infiltration in the *ml3* mutants when compared with the wild type (Fig. 8, C and D). In quantitative terms, this reduced growth was comparable to the reduced growth observed in the *coi1-1* mutant, an established mutant of the *P. syringae* pathogen response (Xie et al., 1998). Based on these observations, we concluded that ML3 has a role in pathogen response in Arabidopsis.

DISCUSSION

In this study, we identify ML3 as a NEDD8- and ubiquitin-modified protein that can be detected in the vacuole and in ER bodies of epidermal cells in Arabidopsis seedlings. ML3 is related to the mammalian proteins MD-2 and NPC2 (Fig. 3; Supplemental Fig. S6). MD-2 recognizes bacterial lipopolysaccharides together with TLR4 as part of the mammalian innate immune response (Viriyakosol et al., 2001; Kim et al., 2007). NPC2 binds to cholesterol in the mammalian lysosome and participates in intracellular cholesterol transport together with the transport protein NPC1 (Frolov et al., 2003; Xu et al., 2007). Thus, ML domain proteins bind to different ligands and localize to diverse cellular compartments. Many ML domain proteins can be

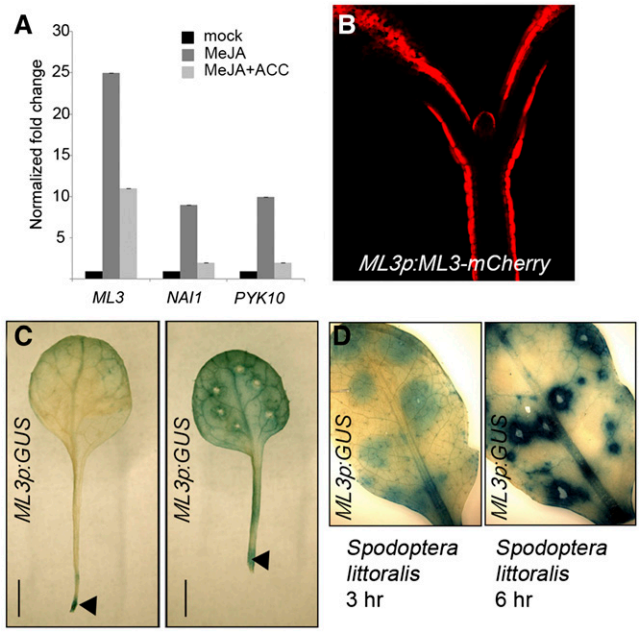

Figure 7. *ML3* expression is regulated by MeJA, ethylene, and wounding. A, Results of qRT-PCR analyses testing for transcript abundance of *ML3*, *NAI1*, and *PYK10* in 16-d-old plants treated for 12 h with a mock solution, MeJA (50 μM), or MeJA and the ethylene precursor 1-aminocyclopropane-1-carboxylic acid (ACC; 50 μM). B, Confocal image of an optical cross section of a 5-d-old seedling expressing *ML3p:ML3-mCherry*. C, Expression analysis of *ML3p:GUS* in the leaves of 16-d-old plants 48 h after wounding with wooden toothpicks (right panel); the left panel shows the mock control. *ML3p:GUS* expression is induced at the sites of toothpick wounding and in the petiole where the leaf was cut off (arrowheads). D, Expression analysis of *ML3p:GUS* in the leaves of 1-month-old plants after feeding by second instar larvae of *S. littoralis*.

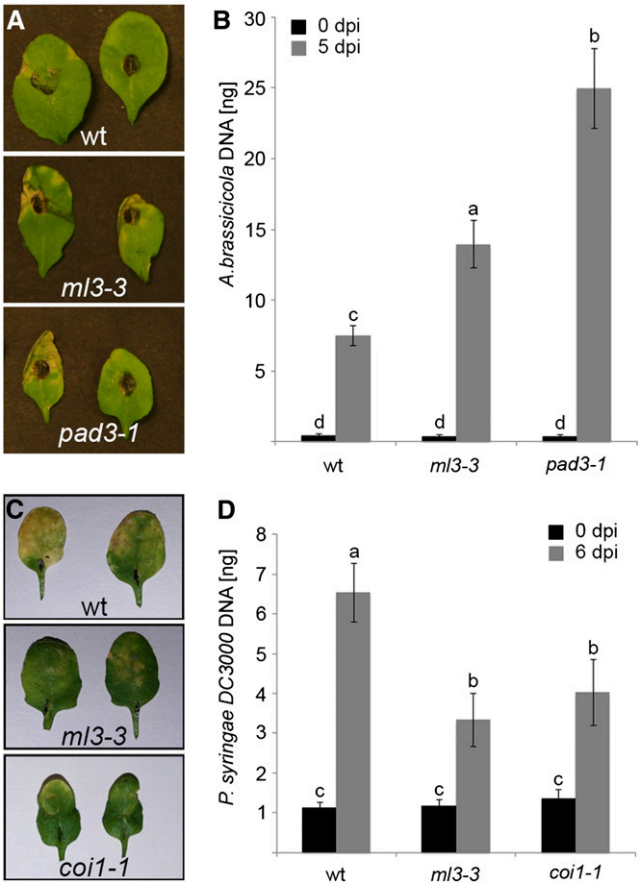

Figure 8. *ml3* mutants are impaired in microbial pathogen responses. A, Representative photographs of leaves from 3-week-old Arabidopsis plants 5 d post infection with 10 μL of a 5 $\times$ 10^5 spores mL^{-1} *A. brassicicola* suspension. B, qRT-PCR analysis for the *A. brassicicola* genomic DNA from 100 mg of plant material as a quantitative measure for fungal growth on infected leaves. C, Representative photographs of leaves from 3-week-old Arabidopsis plants 6 d post infiltration with 10^7 colony-forming units mL^{-1} *P. syringae* DC3000 suspension. D, qRT-PCR analysis of *P. syringae* DC3000 genomic DNA from 100 mg of plant material as a quantitative measure for bacterial growth on infiltrated leaves. dpi, Days post infection; wt, wild type.

identified in the genomes of a variety of plants (Fig. 3), but none of these proteins have been studied at the biochemical or cell biological level to date. Although their overall homology to the better studied mammalian proteins allows suggesting that their biochemical function as binding proteins for a hydrophobic ligand may be conserved, the restricted degree of homology does not allow drawing conclusions on their putative binding partner or transport cargo (Supplemental Fig. S6). Interesting, and possibly also helpful for the identification of candidate ligands for ML3, is the fact that ML3 and its closest homologs appear to form a Brassicales-specific subfamily of ML domain proteins within the larger plant ML protein family (Fig. 3; Supplemental Fig. S5). Thus, also, the ligand of ML3 may be specific for the order Brassicales.

Our cell biological analyses revealed that ML3 is a vacuolar protein that we detected using mCherry fusions of the protein. The vacuolar localization of ML3 could also be confirmed for the endogenous protein in biochemical fractionation experiments. The localization of ML3 to the vacuole is in agreement with the presence of an N-terminal signal peptide that suggests targeting of ML3 to the ER, from where it may be targeted to the vacuole or the secretory pathway (Petersen et al., 2011). This signal peptide is also conserved in the vast majority of ML domain proteins from plants (Fig. 3). The vacuolar localization of ML3 is also in line with the finding that ML3 had previously been reported by others to be a component of the vacuolar proteome (Carter et al., 2004). Thus, similar to mammalian NPC2, ML3 resides in the lysosomal compartment of the cell, where it may retain a specific ligand or participate in a transport process.

We also observed ML3-mCherry and ML3-YFP in ER bodies that were recognizable based on their size and shape in epidermal cells of Arabidopsis seedlings (Fig. 5). Our attempts to confirm the ER body localization for the endogenous ML3 protein by biochemical methods were not successful. This inability to detect endogenous ML3 in ER body fractions using biochemical methods may reflect the fact that ER bodies are only present in epidermis cells and, additionally, represent only a minor fraction of the cellular proteome. Thus, the abundance of ML3 in ER bodies, particularly in comparison with the amount of vacuolar ML3, may be too small to be detected after fractionation on immunoblots with the ML3-specific antibody. For a number of reasons, we consider our observation of the ER body localization of the fluorescent protein-tagged ML3 variants biologically significant. First, *ML3* expression is strongly coregulated with a number of genes that have a known and, in part, demonstrated function in ER body biology, including *NAI1* and *NAI2*, two proteins required for ER body formation (Table I). NAI1 has been proposed to regulate the expression of a number of ER body genes, and *ML3* was previously identified as one of the most strongly down-regulated genes in a gene expression analysis of *nai1* mutants (Nagano et al., 2008). In line with this finding, *ML3* gene expression and protein abundance are strongly reduced in *nai1* mutants, and *ML3* expression follows the dynamics of *NAI1* regulation by MeJA and ethylene (Figs. 6 and 7). *ML3* expression is also coregulated with that of *NAI2*, a protein of unknown biochemical function that is also required for ER body formation (Yamada et al., 2008). Although *nai2* mutants lack ER bodies, ML3 protein is still detectable in this mutant, indicating that ML3 abundance is not dependent on the presence of ER bodies and that the absence of ML3 in *nai1* is most likely the result of the absence of NAI1 as a dominant transcriptional regulator of ML3. In turn, the presence of ER bodies is not affected by the presence or absence of ML3, as revealed by the presence of GFP-HDEL-positive ER bodies in the *ml3-3* mutant (Supplemental Fig. S8). ML3 expression is furthermore coregulated with the β-glucosidase *PYK10/BLU23*, an ER body-specific glucosidase (Sherameti

et al., 2008), the gene encoding MEMBRANE OF ER BODY1 (Yamada et al., 2013), as well as several Jacalin-related lectins and GDSL lipase, which all have been associated with the biology of ER bodies (Nagano et al., 2005, 2008; Yamada et al., 2011). In summary, we conclude that ML3 has a function in ER body biology.

ER bodies have a proposed role in pathogen responses (Yamada et al., 2011). In line with this, we could reveal altered pathogen responses in *ml3* mutants after treatment with the pathogens *A. brassicicola* and *P. syringae* DC3000. Plants often employ distinct recognition mechanisms and signaling pathways for different pathogen elicitors. In this context, the plant hormones SA, JA, or JA/ethylene appear to form a network of synergistic and antagonistic interactions (Glazebrook, 2001; Spoel et al., 2003; Spoel and Dong, 2008; Leon-Reyes et al., 2009). Plants restrict the colonization of some pathogens like *P. syringae* through the elicitation of SA defense responses (Shirasu et al., 1997). Whereas JA-mediated defenses are necessary to inhibit fungal pathogens like *A. brassicicola* (van Wees et al., 2003), in this study, we provide evidence that *ml3-3* mutants are compromised in their JA-mediated defense responses by their enhanced susceptibility toward *A. brassicicola* (Fig. 8A). *P. syringae* is known to suppress SA responses in plants by inducing coronatine-mediated JA signaling (Fig. 8B). The resistant phenotype seen in *ml3* mutants upon *P. syringae* infection is congruent with other studies showing the antagonistic effects of JA and SA signaling (Mur et al., 2006; Spoel et al., 2007; Koornneef et al., 2008).

Interestingly, our results also show that a number of genes of the glucosinolate pathway are strongly coregulated with *ML3*, including the genes for the nitrile specifier proteins NSP1, NSP3, and NSP4 that convert glucosinolates to nitrile (Kuchernig et al., 2012), INDOLE GLUCOSINOLATE *O*-METHYLTRANSFERASE5 (Pfalz et al., 2011), the glucosinolate biosynthesis regulatory transcription factor ATR/MYB34 (score 0.564; Bender and Fink, 1998; Celenza et al., 2005), as well as the ER body marker PYK10 (Sherameti et al., 2008; Table I). Glucosinolate hydrolysis at pH < 5 leads to the formation of nitriles by the activation of the nitrile specifier proteins (Halkier and Gershenzon, 2006; Kissen and Bones, 2009), and in this respect, our observation that a pH shift to 3.5 can lead to changes in the distribution of ML3-mCherry may be biologically significant (Supplemental Fig. S7). PYK10 protein has previously been shown to possess enhanced activity upon hyperinfection by symbiotic fungi by activating toxic compounds such as indole glucosinolates (Ahn et al., 2007; Sherameti et al., 2008). Other studies have revealed that camalexin- and indole glucosinolate-deficient plants are hypersusceptible to the fungus *Sclerotinia sclerotiorum* (Stotz et al., 2011). In addition, JA signaling is essential for the induction of indole glucosinolates (van Dam and Oomen, 2008). Previous studies have shown that *ml3* mutants are compromised in wound-induced JA signaling and are more appetizing for the generalist larva *S. littoralis* (Fridborg et al., 2013). However, plants compromised in *ML3* expression did not show any antiherbivory traits toward the specialist herbivore *Plutella xylostella* (Fridborg et al., 2013). This could be attributed to the fact that *Plutella* spp. have evolved to combat the glucosinolate-myrosinase defense (Kliebenstein et al., 2002). Based on these studies and our observations, we speculate that ML3 is a positive regulator downstream from JA responses and glucosinolate-mediated plant defenses. This suggested link between ML3 and the biology of glucosinolates may also be helpful for the identification of a putative ML3 ligand, which may be a glucosinolate or a glucosinolate-related metabolite, compounds that are known to be stored in the vacuole (Grubb and Abel, 2006).

Our interest in ML3 was triggered following our identification of the protein as a putatively NEDD8-modified protein. ML3 had also been found by others in similar attempts to identify novel NEDD8 conjugates (Hotton et al., 2012). Our experiments now clearly identify a small fraction of ML3 as NEDD8 modified (Fig. 1). Interestingly, we identify also a ubiquitin-conjugated form of ML3 that does not appear to be neddylated, and we are able to show that ML3 can interact with NEDD8 as well as with ubiquitin in the yeast two-hybrid system. Since yeast also contains active neddylation as well as ubiquitylation systems, these interactions may also be the result of conjugation between the respective bait and prey fusion proteins. The modification and binding of both ubiquitin-related proteins to ML3 may be suggestive for a regulatory interplay between these modifier proteins. Unfortunately, we were unable to express and purify ML3 using recombinant expression systems, and this has prevented us from further investigating the interactions between ML3 and the ubiquitin family proteins. Noncovalent interactions of ML3 with NEDD8 and, therefore, an anticipated enrichment of ML3 in purifications of NEDD8 conjugates may be the reason for the identification of ML3 in both proteomics studies aiming at the identification of novel NEDD8 targets from plants (Hakenjos et al., 2011; Hotton et al., 2012). We note that also the ML3-related ML6 was identified unequivocally in our initial MS analysis following HSN purification and that, thus, the findings reported here for ML3 may also apply to the paralogs ML6 and ML5 (Hakenjos et al., 2011; Hotton et al., 2012). Since ML3 does not have any protein features that would be indicative for a binding activity to ubiquitin or ubiquitin-like proteins, these observations as well as the fact that the protein is NEDD8 and ubiquitin modified are very intriguing. At the same time, they give rise to a number of questions about the role and the possible interplay of these modifications and interactions for ML3 biology and function. Future research will have to address these important and exciting issues.

MATERIALS AND METHODS

Biological Material

All experiments were performed in the Arabidopsis (*Arabidopsis thaliana*) ecotype Columbia. Transgenic lines expressing HSN or HSUB were described

previously (Hakenjos et al., 2011). *ml3-3* (SALK_001255) and *ml3-4* (SAIL_182_G07) were obtained from the Nottingham Arabidopsis Stock Centre (NASC) and selected for homozygosity by PCR-based genotyping. *nai1-3* (GK-136G06-012754) is a previously uncharacterized allele of *NAI1*, and *nai2-2* (SALK_005896) and *nai2-3* (SALK_043149) T-DNA insertion mutants were described previously (Yamada et al., 2008). The *nai1* and *nai2* mutant seeds were obtained from NASC and selected for homozygosity by genotyping. *pad3-1* and *coi1-1* are previously published mutants (Xie et al., 1998; Schuhegger et al., 2006). The ER marker lines GFP-HDEL and Q4 were also obtained from NASC (Cutler et al., 2000; Nelson et al., 2007). The transgenic *sp-RFP-AFVY* line was generously provided by Lorenzo Frigerio (University of Warwick). Primer sequences for genotyping are listed in Supplemental Table S1.

Cloning Procedures

To generate MYC-ML3, an *ML3* entry clone (G13160) was obtained from the Arabidopsis Biological Resource Center and then cloned into *pJawohl2B-5xMYC-GW* using Gateway technology (Invitrogen). Mutagenesis of *MYC-ML3* was performed using *Dpn*I-based site-directed mutagenesis with the primers 19 and 20 (*MYC-ML3 K33R*), 21 and 22 (*MYC-ML3 K68R*), 23 and 24 (*MYC-ML3 K90R*), 25 and 26 (*MYC-ML3 K129R*), 27 and 28 (*MYC-ML3 K137R*), 29 and 30 (*MYC-ML3 K147R*), and 31 and 32 (*MYC-ML3 K153R*). ML3-YFP-HA was obtained by insertion of a PCR fragment obtained with primers 11 and 12 into the Gateway-compatible vector *pEarleyGate101* (Earley et al., 2006). The constructs for the expression of the *ML3* promoter-driven ML3-YFP (*ML3p:ML3-YFP*) and ML3-mCherry (*ML3p:ML3-mCherry*) were generated in the following manner. An *ML3* promoter gene fragment was amplified by PCR from Arabidopsis ecotype Columbia genomic DNA with the primers 33 and 35 that added a *Hin*dIII and a *Nhe*I restriction site to the promoter gene termini, respectively. A PCR fragment of the *mCherry* or *YFP* coding sequence flanked by *Nhe*I and *Bam*HI restriction sites was obtained with primers 38 and 39 (*mCherry*) or 40 and 41 (*YFP*), and a 1-kb *ML3* terminator fragment flanked by *Bam*HI and *Xho*I sites was amplified using primers 36 and 37. All fragments were ligated into the *Hin*dIII and *Xho*I restriction sites of *pGreen0029* (*mCherry*) or *pGreen0229* (*YFP*), and the final construct was transformed into the Q4 ER marker line (*ML3p:ML3-mCherry*; Cutler et al., 2000) or *ml3-3* (*ML3p:ML3-YFP*; Hellens et al., 2000).

ML3p:GUS was generated by inserting a 2-kb promoter fragment amplified by PCR (primers 33 and 34) from Arabidopsis Columbia genomic DNA into the vector *pCAMBIA1391Z* (www.cambia.org/daisy/cambia/). At least 10 transgenic Arabidopsis plants were generated for each construct using the floral dip transformation protocol. T1 seeds were selected for resistance to the respective antibiotic or herbicide as well as for transgene expression. Individual lines were chosen for cell biological and biochemical analyses and for genetic crosses. Primer sequences for cloning are listed in Supplemental Table S1.

The yeast two-hybrid construct BD-ML3 was obtained by PCR amplification of the *ML3* open reading frame with oligonucleotides 13 and 14 and was then inserted into *pGBKT7* as an *Eco*RI and *Xho*I fragment. AD-NEDD8 and AD-UBQ were cloned in a similar manner by ligation of the *NEDD8/RUB1* (AT1G31340) and *UBQ* (AT3G52590) open reading frames as *Eco*RI-*Xho*I/*Sal*I fragments into *pGADT7* AD. Primer sequences are listed in Supplemental Table S1.

Quantitative Real-Time PCR

Extraction of total RNA and complementary DNA synthesis were conducted as described previously (Richter et al., 2010). The complementary DNA equivalent of 25 ng of total RNA was used in a 10-μL PCR in a CFX96 Real-Time System Cycler with iQ SYBR Green Supermix (Bio-Rad). A 40-cycle two-step amplification protocol (10 s at 95°C, 30 s at 60°C) was used for all measurements. Primer sequences are listed in Supplemental Table S1. Unless otherwise stated, the average and SE of four technical replicates pooled from at least two biological replicates are shown. The experiment was repeated at least once, and the result of a representative experiment is shown.

Immunobiological Analyses

The anti-ML3 antibody was raised in rabbits by immunization with a chemically synthesized ML3 peptide (VSLRRKTLEED) coupled to a keyhole limpet hemocyanin carrier protein (Eurogentec). The crude serum was affinity purified against the ML3 peptide, and the purified serum was used in a 1:1,000 dilution for immunoblots. Anti-MYC agarose (Roche) and anti-HA agarose (Roche) were used for immunoprecipitations using 1 to 2 g (fresh weight) from 7-d-old seedlings. The anti-NEDD8 antibody (1:1,000) was described previously (Hakenjos et al., 2011). The following commercial antibodies were used: anti-CDC2 (1:3,000; Santa Cruz Biotechnology), anti-GAL4 (DNA-binding domain; 1:1,000; Santa Cruz Biotechnology), anti-GFP (1:3,000; Life Technologies), anti-HA-peroxidase (1:1,000; Roche), and anti-vacuolar-ATPase ε-subunit (1:2,000; Agrisera).

Cell Biological and Histological Analyses

For GUS staining of *ML3p:GUS*, the first and second leaves of 16-d-old plants were wounded using a wooden toothpick and fixed, 48 h after wounding, in heptane for 15 min and then incubated in GUS staining solution [100 mM sodium phosphate buffer (pH 7.0), 2 mM $K_4Fe(CN)_6$, 2 mM $K_3Fe(CN)_6$, 0.1% Triton X-100, and 1 mg mL^{-1} 5-bromo-4-chloro-3-indolyl-β-glucuronic acid]. GUS-stained seedlings were photographed using a Leica MZ16 stereomicroscope with a PLAN-APOX1 objective (Leica). Herbivore feeding experiments with *ML3p:GUS* were performed as described (Fridborg et al., 2013). Microscopy of fluorescent protein fusions was performed on 5-d-old seedlings using an FV1000/IX81 laser-scanning confocal microscope (Olympus).

Subcellular fractionation from 7-d-old seedlings was performed as described previously (Matsushima et al., 2003). Vacuoles were purified from 12- to 14-d-old seedlings using a Ficoll gradient as described previously, and vacuolar proteins were subsequently precipitated using TCA (Robert et al., 2007).

MS

For protein digestion, a sample of immunoprecipitated ML3-YFP-HA was reduced and alkylated by 50 mM dithiothreitol and 10 mg mL^{-1} chloroacetamide, respectively. Tryptic in-gel digestion was performed according to standard procedures. Nanoflow liquid chromatography-tandem MS was performed using an Eksigent nanoLC-Ultra 1D+ system coupled online to an LTQ-Orbitrap Velos (Thermo Scientific) mass spectrometer. Tryptic peptides were dissolved in 20 μL of buffer A (0.1% formic acid in double-distilled water), and 10 μL was injected for each measurement. Peptide samples were first loaded on a trap column (100 μm i.d. $\times$ 2 cm, packed in house with 5 μm Reprosil PUR AQ; Dr. Maisch) in 100% buffer A. Peptides were transferred to an analytical column (75-μm $\times$ 40-cm C18 column, 3 μm Reprosil PUR AQ Gold; Dr. Maisch) and separated using a 225-min gradient from 7% to 35% buffer B (0.1% formic acid in acetonitrile). MS measurements were performed in data-dependent acquisition mode, automatically subjecting the 10 most abundant precursor ions in the full MS spectra for higher-energy collisional dissociation fragmentation at 30% collision energy. Full MS spectra and tandem MS spectra were acquired at 30,000 and 7,500 resolution, respectively. Intensity-based label-free quantification was performed using Progenesis (version 4.0; Nonlinear Dynamics). The generated peak list was then searched using Mascot (version 2.4.1) against the protein sequence databases National Center for Biotechnology Information non-redundant (download October 26, 2011; 15.8 million sequences) and SwissProt (version 57; 0.5 million sequences) for protein identification. The variable modification of Lys(GlyGly) was considered in the database search in order to identify NEDD8-modified ML3.

Phylogenetic Analysis

Protein sequences containing the MD-2-related lipid-recognition domain (PF02221) were retrieved from the Ensembl BioMart database for the dicot species Arabidopsis, *Brassica rapa*, soybean (*Glycine max*), tomato (*Solanum lycopersicum*), and grapevine (*Vitis vinifera*), the monocot species *Brachypodium distachyon* and rice (*Oryza sativa*), as well as the moss *Physcomitrella patens* and the lycophyte *Selaginella moellendorffii*. Sequences were aligned with ClustalOmega (www.ebi.ac.uk/Tools/msa/clustalo/) and manually amended when necessary. The phylogenetic tree was constructed based on the amended alignment with MEGA5 using the maximum likelihood method and the bootstrap method with 1,000 bootstrap replications. The tree was rooted with the sequences from *P. patens* and *S. moellendorffii*. The cutoff values for the bootstrap analysis were set to 60%, and bootstrap values are indicated by each node.

Genevestigator

A list of 20 genes coexpressed with *ML3* was generated on the basis of 8,689 Affymetrix 22k ATH1 microarray samples using the Genevestigator coexpression tool (www.genevestigator.com).

Chemical Treatments

To examine the effects of MeJA and ethylene on *ML3* expression, rosette leaves of 16-d-old plants were floated for 12 h on water containing 50 μM MeJA. The ethylene precursor 1-aminocyclopropane-1-carboxylic acid (50 μM) was added for the combined treatments with MeJA and ethylene. To examine the cellular distribution of ML3-mCherry and RFP-AVFY, 5-d-old seedlings were treated for 2 h with SA (500 μM), 3-hydroxybenzoic acid (500 μM) dissolved in water, germination medium (4.3 g L^{-1} Murashige and Skoog medium, 10 g L^{-1} saccharose, and 0.5 g L^{-1} MES, pH 5.8) or 0.5 M mannitol or, alternatively, in water, pH 3.5 (HCl). Dexamethasone-inducible transgenes were induced by immersing the plant material overnight in liquid germination medium supplemented with 30 μM dexamethasone (Sigma; Aoyama and Chua, 1997).

Yeast Two-Hybrid Assay

The yeast two-hybrid assay was performed as described previously (Katsiarimpa et al., 2011).

Pathogen Assays

Alternaria brassicicola strain MUCL20297 was grown on potato dextrose agar plates for 2 weeks at 22°C. Spores were then harvested and suspended in water (5×10^5 spores mL^{-1}). *A. brassicicola* inoculation was performed by adding 5-μL drops onto the leaf surface as described previously (Thomma et al., 1998). Two leaves per plant were inoculated with two drops each. Ten plants were taken as one biological replicate, and three biological replicates were used. Five days after challenge, disease severity was scored and samples were collected for pathogen quantification. Disease rating was assessed on the basis of symptom severity (Van der Ent et al., 2008). For each pathogen assay, inoculated leaves of 10 plants were pooled together and taken as one biological replicate, and three biological replicates were used. Fungal DNA quantification was carried out by quantitative real-time (qRT)-PCR of ABU03393 using the primers 48 and 49. In preparation for a *Pseudomonas syringae* pv *tomato* DC3000 experiment, the bacteria were grown overnight in Luria-Bertani medium at 37°C. The cells were centrifuged, and the pellet was washed once with sterile 10 mM $MgCl_2$ and resuspended in 10 mM $MgCl_2$ to an optical density at 600 nm of 0.02 (10^7 colony-forming units mL^{-1}). Inoculations for the *P. syringae* pv *tomato* DC3000 bioassays were performed through pressure infiltration with bacterial suspension into the tissue of the abaxial part of the rosette leaves (two leaves per plant). About 100 μL of suspension was used for each leaf, and 10 plants were infiltrated for one biological replicate. Three biological replicates were used in the study. The experiment was carried out twice, and a representative experiment is shown. Pathogen quantification for *P. syringae* pv *tomato* DC3000 was performed by qRT-PCR of NC_004578 using the primers 50 and 51.

Sequence data from this article can be found in the GenBank/EMBL data libraries under accession numbers: *ML3* (AT5G23820), *NEDD8* (AT1G31340), *NAI1* (AT2G22770), *NAI2* (AT3G15950), *PYK10* (AT3G09260), *COI1* (AT2G39940), and *PAD3* (AT3G26830). GenBank accession numbers of human genes mentioned in this work are *MD-2* (AB018549), *MD-1* (AF057178), *NPC2* (NM_006432) and *GM2A* (NM_000405).

Supplemental Data

The following materials are available in the online version of this article.

Supplemental Figure S1. Mass spectrometric analysis of ML3.

Supplemental Figure S2. Mutational analysis of MYC-ML3 protein.

Supplemental Figure S3. MLN4924 blocks NEDD8-modification of ML3.

Supplemental Figure S4. HSN-immunoprecipitates recover ML3.

Supplemental Figure S5. Protein alignment of the ML domain used for the phylogeny.

Supplemental Figure S6. Protein sequence alignment of ML3 with human and Arabidopsis ML domain proteins.

Supplemental Figure S7. Acidic pH causes relocalization of vacuolar proteins.

Supplemental Figure S8. ER body formation is unaltered in *ml3-3* mutants.

Supplemental Table S1. List of primers.

ACKNOWLEDGMENTS

We thank Ralph Hückelhoven (Technische Universität München) and Erich Glawischnig (Technische Universität München) for their expert advice. We thank Susan Kläger (Technische Universität München) for technical assistance.

Received May 13, 2013; accepted July 30, 2013; published July 31, 2013.

LITERATURE CITED

Ahn YO, Shimizu B, Sakata K, Gantulga D, Zhou C, Bevan DR, Esen A (2010) Scopolin-hydrolyzing beta-glucosidases in roots of Arabidopsis. Plant Cell Physiol **51:** 132–143

Ahn YO, Zheng M, Bevan DR, Esen A, Shiu SH, Benson J, Peng HP, Miller JT, Cheng CL, Poulton JE, et al (2007) Functional genomic analysis of Arabidopsis thaliana glycoside hydrolase family 35. Phytochemistry **68:** 1510–1520

Aoyama T, Chua NH (1997) A glucocorticoid-mediated transcriptional induction system in transgenic plants. Plant J **11:** 605–612

Bejai S, Fridborg I, Ekbom B (2012) Varied response of Spodoptera littoralis against Arabidopsis thaliana with metabolically engineered glucosinolate profiles. Plant Physiol Biochem **50:** 72–78

Bender J, Fink GR (1998) A Myb homologue, ATR1, activates tryptophan gene expression in Arabidopsis. Proc Natl Acad Sci USA **95:** 5655–5660

Bonnett HT Jr, Newcomb EH (1965) Polyribosomes and cisternal accumulations in root cells of radish. J Cell Biol **27:** 423–432

Carter C, Pan S, Zouhar J, Avila EL, Girke T, Raikhel NV (2004) The vegetative vacuole proteome of *Arabidopsis thaliana* reveals predicted and unexpected proteins. Plant Cell **16:** 3285–3303

Celenza JL, Quiel JA, Smolen GA, Merrikh H, Silvestro AR, Normanly J, Bender J (2005) The Arabidopsis ATR1 Myb transcription factor controls indolic glucosinolate homeostasis. Plant Physiol **137:** 253–262

Cutler SR, Ehrhardt DW, Griffitts JS, Somerville CR (2000) Random GFP: cDNA fusions enable visualization of subcellular structures in cells of Arabidopsis at a high frequency. Proc Natl Acad Sci USA **97:** 3718–3723

del Pozo JC, Dharmasiri S, Hellmann H, Walker L, Gray WM, Estelle M (2002) AXR1-ECR1-dependent conjugation of RUB1 to the Arabidopsis cullin AtCUL1 is required for auxin response. Plant Cell **14:** 421–433

del Pozo JC, Estelle M (1999) The Arabidopsis cullin AtCUL1 is modified by the ubiquitin-related protein RUB1. Proc Natl Acad Sci USA **96:** 15342–15347

del Pozo JC, Timpte C, Tan S, Callis J, Estelle M (1998) The ubiquitin-related protein RUB1 and auxin response in Arabidopsis. Science **280:** 1760–1763

Deshaies RJ, Joazeiro CA (2009) RING domain E3 ubiquitin ligases. Annu Rev Biochem **78:** 399–434

Duda DM, Borg LA, Scott DC, Hunt HW, Hammel M, Schulman BA (2008) Structural insights into NEDD8 activation of cullin-RING ligases: conformational control of conjugation. Cell **134:** 995–1006

Duda DM, Scott DC, Calabrese MF, Zimmerman ES, Zheng N, Schulman BA (2011) Structural regulation of cullin-RING ubiquitin ligase complexes. Curr Opin Struct Biol **21:** 257–264

Earley KW, Haag JR, Pontes O, Opper K, Juehne T, Song K, Pikaard CS (2006) Gateway-compatible vectors for plant functional genomics and proteomics. Plant J **45:** 616–629

Fridborg I, Johansson A, Lagensjö J, Leelarasamee N, Floková K, Tarkowská D, Meijer J, Bejai S (2013) ML3: a novel regulator of herbivory-induced responses in Arabidopsis thaliana. J Exp Bot **64:** 935–948

Frolov A, Zielinski SE, Crowley JR, Dudley-Rucker N, Schaffer JE, Ory DS (2003) NPC1 and NPC2 regulate cellular cholesterol homeostasis through generation of low density lipoprotein cholesterol-derived oxysterols. J Biol Chem **278:** 25517–25525

Glazebrook J (2001) Genes controlling expression of defense responses in Arabidopsis: 2001 status. Curr Opin Plant Biol **4:** 301–308

Grubb CD, Abel S (2006) Glucosinolate metabolism and its control. Trends Plant Sci **11:** 89–100

Hakenjos JP, Richter R, Dohmann EM, Katsiarimpa A, Isono E, Schwechheimer C (2011) MLN4924 is an efficient inhibitor of NEDD8 conjugation in plants. Plant Physiol **156:** 527–536

Halkier BA, Gershenzon J (2006) Biology and biochemistry of glucosinolates. Annu Rev Plant Biol **57:** 303–333

Hara-Nishimura I, Matsushima R (2003) A wound-inducible organelle derived from endoplasmic reticulum: a plant strategy against environmental stresses? Curr Opin Plant Biol **6:** 583–588

Harper JW, Tan MK (2012) Understanding cullin-RING E3 biology through proteomics-based substrate identification. Mol Cell Proteomics **11:** 1541–1550

Haseloff J, Siemering KR, Prasher DC, Hodge S (1997) Removal of a cryptic intron and subcellular localization of green fluorescent protein are required to mark transgenic Arabidopsis plants brightly. Proc Natl Acad Sci USA **94:** 2122–2127

Hayashi Y, Yamada K, Shimada T, Matsushima R, Nishizawa NK, Nishimura M, Hara-Nishimura I (2001) A proteinase-storing body that prepares for cell death or stresses in the epidermal cells of Arabidopsis. Plant Cell Physiol **42:** 894–899

Hellens RP, Edwards EA, Leyland NR, Bean S, Mullineaux PM (2000) pGreen: a versatile and flexible binary Ti vector for Agrobacterium-mediated plant transformation. Plant Mol Biol **42:** 819–832

Hotton SK, Callis J (2008) Regulation of cullin RING ligases. Annu Rev Plant Biol **59:** 467–489

Hotton SK, Castro MF, Eigenheer RA, Callis J (2012) Recovery of DDB1a (damaged DNA binding protein1a) in a screen to identify novel RUB-modified proteins in Arabidopsis thaliana. Mol Plant **5:** 1163–1166

Hunter PR, Craddock CP, Di Benedetto S, Roberts LM, Frigerio L (2007) Fluorescent reporter proteins for the tonoplast and the vacuolar lumen identify a single vacuolar compartment in Arabidopsis cells. Plant Physiol **145:** 1371–1382

Inohara N, Nuñez G (2002) ML: a conserved domain involved in innate immunity and lipid metabolism. Trends Biochem Sci **27:** 219–221

Katsiarimpa A, Anzenberger F, Schlager N, Neubert S, Hauser MT, Schwechheimer C, Isono E (2011) The *Arabidopsis* deubiquitinating enzyme AMSH3 interacts with ESCRT-III subunits and regulates their localization. Plant Cell **23:** 3026–3040

Kim HM, Park BS, Kim JI, Kim SE, Lee J, Oh SC, Enkhbayar P, Matsushima N, Lee H, Yoo OJ, et al (2007) Crystal structure of the TLR4-MD-2 complex with bound endotoxin antagonist Eritoran. Cell **130:** 906–917

Kissen R, Bones AM (2009) Nitrile-specifier proteins involved in glucosinolate hydrolysis in Arabidopsis thaliana. J Biol Chem **284:** 12057–12070

Kliebenstein D, Pedersen D, Barker B, Mitchell-Olds T (2002) Comparative analysis of quantitative trait loci controlling glucosinolates, myrosinase and insect resistance in Arabidopsis thaliana. Genetics **161:** 325–332

Komander D, Clague MJ, Urbé S (2009) Breaking the chains: structure and function of the deubiquitinases. Nat Rev Mol Cell Biol **10:** 550–563

Komander D, Rape M (2012) The ubiquitin code. Annu Rev Biochem **81:** 203–229

Koornneef A, Leon-Reyes A, Ritsema T, Verhage A, Den Otter FC, Van Loon LC, Pieterse CM (2008) Kinetics of salicylate-mediated suppression of jasmonate signaling reveal a role for redox modulation. Plant Physiol **147:** 1358–1368

Kuchernig JC, Burow M, Wittstock U (2012) Evolution of specifier proteins in glucosinolate-containing plants. BMC Evol Biol **12:** 127

Leon-Reyes A, Spoel SH, De Lange ES, Abe H, Kobayashi M, Tsuda S, Millenaar FF, Welschen RA, Ritsema T, Pieterse CM (2009) Ethylene modulates the role of NONEXPRESSOR OF PATHOGENESIS-RELATED GENES1 in cross talk between salicylate and jasmonate signaling. Plant Physiol **149:** 1797–1809

Ma T, Chen Y, Zhang F, Yang CY, Wang S, Yu X (2013) RNF111-dependent neddylation activates DNA damage-induced ubiquitination. Mol Cell **49:** 897–907

Mahata B, Sundqvist A, Xirodimas DP (2012) Recruitment of RPL11 at promoter sites of p53-regulated genes upon nucleolar stress through NEDD8 and in an Mdm2-dependent manner. Oncogene **31:** 3060–3071

Matsushima R, Fukao Y, Nishimura M, Hara-Nishimura I (2004) *NAI1* gene encodes a basic-helix-loop-helix-type putative transcription factor that regulates the formation of an endoplasmic reticulum-derived structure, the ER body. Plant Cell **16:** 1536–1549

Matsushima R, Hayashi Y, Kondo M, Shimada T, Nishimura M, Hara-Nishimura I (2002) An endoplasmic reticulum-derived structure that is induced under stress conditions in Arabidopsis. Plant Physiol **130:** 1807–1814

Matsushima R, Kondo M, Nishimura M, Hara-Nishimura I (2003) A novel ER-derived compartment, the ER body, selectively accumulates a beta-glucosidase with an ER-retention signal in Arabidopsis. Plant J **33:** 493–502

Mur LA, Kenton P, Atzorn R, Miersch O, Wasternack C (2006) The outcomes of concentration-specific interactions between salicylate and jasmonate signaling include synergy, antagonism, and oxidative stress leading to cell death. Plant Physiol **140:** 249–262

Nagano AJ, Fukao Y, Fujiwara M, Nishimura M, Hara-Nishimura I (2008) Antagonistic jacalin-related lectins regulate the size of ER body-type beta-glucosidase complexes in Arabidopsis thaliana. Plant Cell Physiol **49:** 969–980

Nagano AJ, Maekawa A, Nakano RT, Miyahara M, Higaki T, Kutsuna N, Hasezawa S, Hara-Nishimura I (2009) Quantitative analysis of ER body morphology in an Arabidopsis mutant. Plant Cell Physiol **50:** 2015–2022

Nagano AJ, Matsushima R, Hara-Nishimura I (2005) Activation of an ER-body-localized beta-glucosidase via a cytosolic binding partner in damaged tissues of Arabidopsis thaliana. Plant Cell Physiol **46:** 1140–1148

Nelson BK, Cai X, Nebenführ A (2007) A multicolored set of in vivo organelle markers for co-localization studies in Arabidopsis and other plants. Plant J **51:** 1126–1136

Noh EH, Hwang HS, Hwang HS, Min B, Im E, Chung KC (2012) Covalent NEDD8 conjugation increases RCAN1 protein stability and potentiates its inhibitory action on calcineurin. PLoS ONE **7:** e48315

Ogasawara K, Yamada K, Christeller JT, Kondo M, Hatsugai N, Hara-Nishimura I, Nishimura M (2009) Constitutive and inducible ER bodies of Arabidopsis thaliana accumulate distinct beta-glucosidases. Plant Cell Physiol **50:** 480–488

Oh IS, Park AR, Bae MS, Kwon SJ, Kim YS, Lee JE, Kang NY, Lee S, Cheong H, Park OK (2005) Secretome analysis reveals an *Arabidopsis* lipase involved in defense against *Alternaria brassicicola*. Plant Cell **17:** 2832–2847

Park BS, Song DH, Kim HM, Choi BS, Lee H, Lee JO (2009) The structural basis of lipopolysaccharide recognition by the TLR4-MD-2 complex. Nature **458:** 1191–1195

Petersen TN, Brunak S, von Heijne G, Nielsen H (2011) SignalP 4.0: discriminating signal peptides from transmembrane regions. Nat Methods **8:** 785–786

Pfalz M, Mikkelsen MD, Bednarek P, Olsen CE, Halkier BA, Kroymann J (2011) Metabolic engineering in *Nicotiana benthamiana* reveals key enzyme functions in *Arabidopsis* indole glucosinolate modification. Plant Cell **23:** 716–729

Praefcke GJ, Hofmann K, Dohmen RJ (2012) SUMO playing tag with ubiquitin. Trends Biochem Sci **37:** 23–31

Rabut G, Peter M (2008) Function and regulation of protein neddylation. 'Protein modifications: beyond the usual suspects' review series. EMBO Rep **9:** 969–976

Richter R, Behringer C, Müller IK, Schwechheimer C (2010) The GATA-type transcription factors GNC and GNL/CGA1 repress gibberellin signaling downstream from DELLA proteins and PHYTOCHROME-INTERACTING FACTORS. Genes Dev **24:** 2093–2104

Ridge RW, Uozumi Y, Plazinski J, Hurley UA, Williamson RE (1999) Developmental transitions and dynamics of the cortical ER of Arabidopsis cells seen with green fluorescent protein. Plant Cell Physiol **40:** 1253–1261

Robert S, Zouhar J, Carter C, Raikhel N (2007) Isolation of intact vacuoles from Arabidopsis rosette leaf-derived protoplasts. Nat Protoc **2:** 259–262

Schuhegger R, Nafisi M, Mansourova M, Petersen BL, Olsen CE, Svatos A, Halkier BA, Glawischnig E (2006) CYP71B15 (PAD3) catalyzes the final step in camalexin biosynthesis. Plant Physiol **141:** 1248–1254

Sherameti I, Venus Y, Drzewiecki C, Tripathi S, Dan VM, Nitz I, Varma A, Grundler FM, Oelmüller R (2008) PYK10, a beta-glucosidase located in the endoplasmatic reticulum, is crucial for the beneficial interaction between Arabidopsis thaliana and the endophytic fungus Piriformospora indica. Plant J **54:** 428–439

Shirasu K, Nakajima H, Rajasekhar VK, Dixon RA, Lamb C (1997) Salicylic acid potentiates an agonist-dependent gain control that amplifies pathogen signals in the activation of defense mechanisms. Plant Cell **9:** 261–270

Spoel SH, Dong X (2008) Making sense of hormone crosstalk during plant immune responses. Cell Host Microbe **3:** 348–351

Spoel SH, Johnson JS, Dong X (2007) Regulation of tradeoffs between plant defenses against pathogens with different lifestyles. Proc Natl Acad Sci USA **104:** 18842–18847

Spoel SH, Koornneef A, Claessens SM, Korzelius JP, Van Pelt JA, Mueller MJ, Buchala AJ, Métraux JP, Brown R, Kazan K, et al (2003) NPR1 modulates

cross-talk between salicylate- and jasmonate-dependent defense pathways through a novel function in the cytosol. Plant Cell **15:** 760–770

Stotz HU, Sawada Y, Shimada Y, Hirai MY, Sasaki E, Krischke M, Brown PD, Saito K, Kamiya Y (2011) Role of camalexin, indole glucosinolates, and side chain modification of glucosinolate-derived isothiocyanates in defense of Arabidopsis against Sclerotinia sclerotiorum. Plant J **67:** 81–93

Tamura K, Shimada T, Ono E, Tanaka Y, Nagatani A, Higashi SI, Watanabe M, Nishimura M, Hara-Nishimura I (2003) Why green fluorescent fusion proteins have not been observed in the vacuoles of higher plants. Plant J **35:** 545–555

Thomma BP, Eggermont K, Penninckx IA, Mauch-Mani B, Vogelsang R, Cammue BP, Broekaert WF (1998) Separate jasmonate-dependent and salicylate-dependent defense-response pathways in Arabidopsis are essential for resistance to distinct microbial pathogens. Proc Natl Acad Sci USA **95:** 15107–15111

van Dam NM, Oomen MW (2008) Root and shoot jasmonic acid applications differentially affect leaf chemistry and herbivore growth. Plant Signal Behav **3:** 91–98

Van der Ent S, Verhagen BW, Van Doorn R, Bakker D, Verlaan MG, Pel MJ, Joosten RG, Proveniers MC, Van Loon LC, Ton J, et al (2008) *MYB72* is required in early signaling steps of rhizobacteria-induced systemic resistance in Arabidopsis. Plant Physiol **146:** 1293–1304

van Wees SC, Chang HS, Zhu T, Glazebrook J (2003) Characterization of the early response of Arabidopsis to *Alternaria brassicicola* infection using expression profiling. Plant Physiol **132:** 606–617

Vierstra RD (2012) The expanding universe of ubiquitin and ubiquitin-like modifiers. Plant Physiol **160:** 2–14

Viriyakosol S, Tobias PS, Kitchens RL, Kirkland TN (2001) MD-2 binds to bacterial lipopolysaccharide. J Biol Chem **276:** 38044–38051

Woodward AW, Ratzel SE, Woodward EE, Shamoo Y, Bartel B (2007) Mutation of *E1-CONJUGATING ENZYME-RELATED1* decreases RELATED TO UBIQUITIN conjugation and alters auxin response and development. Plant Physiol **144:** 976–987

Xie DX, Feys BF, James S, Nieto-Rostro M, Turner JG (1998) COI1: an Arabidopsis gene required for jasmonate-regulated defense and fertility. Science **280:** 1091–1094

Xirodimas DP (2008) Novel substrates and functions for the ubiquitin-like molecule NEDD8. Biochem Soc Trans **36:** 802–806

Xirodimas DP, Saville MK, Bourdon JC, Hay RT, Lane DP (2004) Mdm2-mediated NEDD8 conjugation of p53 inhibits its transcriptional activity. Cell **118:** 83–97

Xirodimas DP, Sundqvist A, Nakamura A, Shen L, Botting C, Hay RT (2008) Ribosomal proteins are targets for the NEDD8 pathway. EMBO Rep **9:** 280–286

Xu S, Benoff B, Liou HL, Lobel P, Stock AM (2007) Structural basis of sterol binding by NPC2, a lysosomal protein deficient in Niemann-Pick type C2 disease. J Biol Chem **282:** 23525–23531

Yamada K, Hara-Nishimura I, Nishimura M (2011) Unique defense strategy by the endoplasmic reticulum body in plants. Plant Cell Physiol **52:** 2039–2049

Yamada K, Nagano AJ, Nishina M, Hara-Nishimura I, Nishimura M (2008) NAI2 is an endoplasmic reticulum body component that enables ER body formation in *Arabidopsis thaliana*. Plant Cell **20:** 2529–2540

Yamada K, Nagano AJ, Nishina M, Hara-Nishimura I, Nishimura M (2013) Identification of two novel endoplasmic reticulum body-specific integral membrane proteins. Plant Physiol **161:** 108–120

Yamada K, Nagano AJ, Ogasawara K, Hara-Nishimura I, Nishimura M (2009) The ER body, a new organelle in Arabidopsis thaliana, requires NAI2 for its formation and accumulates specific beta-glucosidases. Plant Signal Behav **4:** 849–852